Chapter 4.7. Thermodynamic analysis of the autothermal partial oxidation/steam reforming of ethanol by MeO (Me = Ni, Cu) with CO_2 capture

V. Collins-Martínez; M. J. Meléndez-Zaragoza; A. López-Ortiz*

Departamento de Ingeniería y Química de Materiales, Centro de Investigación en Materiales Avanzados, S.C., Miguel de Cervantes 120, Chihuahua, Chih., México, 31136, México.

ABSTRACT

Hydrogen is generally considered as a clean and high efficient energy carrier that can be employed for power generation through fuel cell units, with innocuous water as the only by-product, to decrease the release of pollutants into the atmosphere. Today, there is a developing interest for hydrogen generation from renewable sources such as bio-oil, bio-gas, bio-ethanol or bio-butanol etc. Among the different renewable feedstock options, ethanol has been viewed as an appealing feedstock because of its relatively high hydrogen content, accessibility, nontoxicity, ease of handling and safety. The present thermodynamic analysis is aimed to explore autothermal conditions at equilibrium for a high H_2-syngas production under the combined ethanol steam reforming (SRE), chemical looping partial oxidation (CLPOX) and CO_2 solid absorption reaction system. SRE studied conditions were H_2O/C_2H_6O = 3-6 molar ratio, CLPOX employed NiO or CuO as metal oxide (MeO) oxygen carriers from MeO/C_2H_6O = 0.05-1.5 molar ratio, while 2 kmols of CaO were used for CO_2 capture in a T range of 100-900 °C at 1 atm. NiO most favorable adiabatic conditions (T ≥ 500 °C and C ≤ 0.1 kmols) were: H_2O/C_2H_6O = 3 and NiO/C_2H_6O = 0.05-0.5. While, for CuO was at H_2O/C_2H_6O = 4, CuO/C_2H_6O = 0.5 and T_{adiab} = 529 °C. These favorable reaction conditions are the product of the combination of the exothermic carbonation reaction and its influence over the thermodynamic equilibrium over the POX and SRE endothermic reactions.

Keywords: Combined SRE CLPOX and CO_2 capture, Autothermal thermodynamic conditions

1. Introduction

Hydrogen is generally considered as a clean and high efficient energy carrier that can be employed for power generation through fuel cell units, with innocuous water as the only by-product, to decrease the release of pollutants into the atmosphere [1]. Hydrogen presents an energy content of 143 MJ/kg, which is approximately three times higher than any liquid

----

* Author for correspondence:
Dr. Alejandro López-Ortiz, T:52 614 4394815, E: alejandro.lopez@cimav.edu.mx

hydrocarbon based fuel [2]. Furthermore, other benefits for hydrogen utilization are plenty availability, use of a wide diversity of feedstocks and a variety of production technologies [3]. Other uses of hydrogen include the manufacture of ammonia and other fertilizers (e.g. urea), to upgrade heavy oils, and to produce a wide variety of chemicals and fuels.

Currently, new approaches are being investigated in order to produce hydrogen in a mass scale such as water electrolysis, hydrocarbon reforming, photocatalytic water splitting and biological processes etc [4-6]. Nevertheless, steam reforming of fossil based hydrocarbons, mainly natural gas, is the most common process for hydrogen production worldwide, but generally ignoring the high costs in terms of damage to the environment [7]. Furthermore, the use of fossil fuels for supplementary energy production is non-sustainable.

Considering the sustainable advance, there is a developing interest for hydrogen generation from renewable sources such as bio-oil, bio-gas, bio-ethanol or bio-butanol etc. [8]. Among the different renewable feedstock options, ethanol has been viewed as an appealing feedstock because of its relatively high hydrogen content, accessibility, nontoxicity, ease of handling and safety [9].

Moreover, steam reforming (SR), partial oxidation (POX) and autothermal steam reforming (ATR) are the most important studied processes for hydrogen production from ethanol.

$$C_2H_5OH + 3H_2O \longrightarrow 6H_2 + 2CO_2 \qquad\qquad \Delta H^0 = 173.3 \text{ kJ/mol} \qquad\qquad (1)$$

Ethanol SR (Eq. (1)) is the most widely studied route since it generates the highest hydrogen yield. This process is typically considered as a combination of ethanol SR to syngas followed by water–gas shift (WGS, Eq. 2).

$$CO + H_2O \longrightarrow H_2 + CO_2 \qquad\qquad \Delta H^0 = -41.138 \text{ kJ/mol} \qquad\qquad (2)$$

Thermodynamic analysis indicates that equilibrium H_2 yield can be as high as 70 mol% for ethanol SR at 700 °C with a stoichiometric molar feed ratio (H_2O/C_2H_5OH) of 3 [10,11]. However, ethanol SR is highly endothermic, demanding a large amount of energy, which increases operating costs. This serious disadvantage significantly hinders the practical hydrogen production, particularly for on-board applications.

$$C_2H_5OH + 1.5O_2 \longrightarrow 3H_2 + 2CO_2 \qquad\qquad \Delta H^0 = -552.2 \text{ kJ/mol} \qquad\qquad (3)$$

POX of ethanol (reaction 3) is an alternative process for hydrogen production. Compared to ethanol SR, POX is exothermic and fast, and very appropriate for handling rapid loading variations, such as those usually demanded by on-board reformers, which frequently perform under variable conditions. In the meantime, benefits of this oxidative process are its lower reaction temperature and fewer tendency for carbon formation due to the oxygen addition. Though, an excess in oxygen content oxidation may lead to lower hydrogen yield compared to the SR process.

$$C_2H_5OH + 1.8H_2O + 0.6O_2 \longrightarrow 4.8\ H_2 + 2CO_2 \qquad \Delta H^0 = -116.9 \text{ kJ/mol} \qquad (4)$$

ATR of ethanol, is a combination of SR and POX represents a compromise between energy efficiency and hydrogen yield. Oxygen from the feed may provide the necessary heat for the endothermic ethanol SR due to the exothermic nature of the partial oxidation of ethanol [12].

Therefore, with a stoichiometric feed ratio ($H_2O/C_2H_5OH/O_2$ = 3/1/0.6), the overall reaction can be thermally neutral (ΔH^0 =+4.4 kJ/mol) and the dry H_2 content can reach ~70 mol% in the product stream [13]. This means that ethanol ATR not only alleviate the heat demand of the system, but leads to a reasonably high hydrogen yield. Moreover, the presence of oxygen also eases the removal of carbon deposition formed during the reactor operation.

Thermodynamic analysis of ethanol SR process shows high values of equilibrium constant for temperatures above 323 °C and an increase in temperature prevents methane formation (the main byproduct consuming H_2) [14]. Increasing space time enhances the ethanol conversion and hydrogen selectivity together with the reduction of the intermediates formation [15]. In general, an increase in water in the reactants favors the ethanol conversion and H_2 production. The increase of CO_2 concentration together with the decrease of CO implies that the addition of water also promotes the WGS reaction. The presence of oxygen in the feed may promote the initial ethanol conversion. However, H_2 concentration decreased due to the partial oxidation. Moreover, coke formation significantly reduces with the increase in H_2O/C_2H_5OH or O_2/C_2H_5OH ratios considering the contribution of the carbon gasification by H_2O or O_2. ATR is a convenient reaction for the on-board H_2 production for portable applications requiring high H_2 selectivity and fast response (startup). With suitable precursors and process control, the ATR has been used for the production of other chemicals as well [16]. However, one of the main disadvantages of this ATR reaction system is the need for a pure source of O_2.

Moreover, chemical looping partial oxidation (CLPOX) is a novel POX process that avoids the use of pure O_2 consumption [17]. In this process the O_2/fuel ratio is kept low to prevent complete oxidation to CO_2 and H_2O. This CLPOX process makes possible to obtain a N_2 free Syngas from the POX reactor avoiding the O_2/N_2 separation step in the conventional POX process. This CLPOX process involves the use of an oxygen carrier, which transfers oxygen from air to the fuel, avoiding the direct contact between them. This process is composed of two interconnected reactors; a fuel reactor (I) and an air reactor (II), as described in Figure 1. In the fuel reactor a hydrocarbon-based fuel (ethanol) is partially oxidized to produce Syngas (CO + H_2) by a metal oxide (MeO) that is reduced to a metallic state (Me) or to a reduced form of the MeO. The metal or reduced oxide (Me) is further transferred to the air reactor where it is oxidized back to MeO with air, and the regenerated material is then sent back to the fuel reactor to start a new cycle. The flue gas leaving the air reactor contains N_2 and unreacted O_2, while the exit gases from the fuel reactor contains Syngas, CO_2 and H_2O.
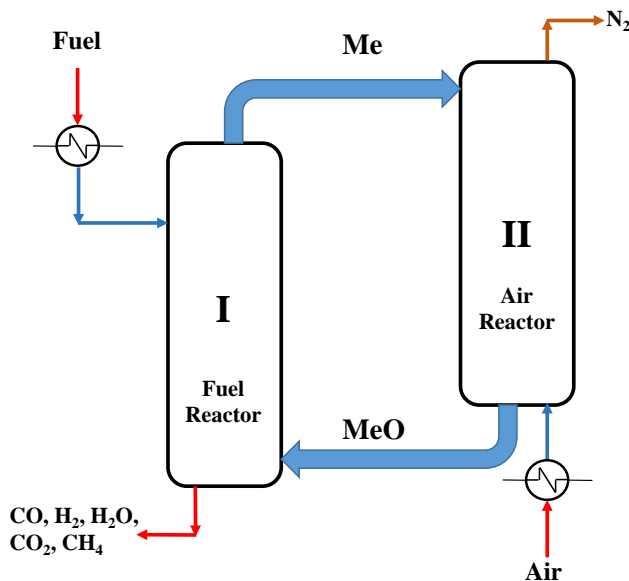
Fig. 1. Conceptual design of CLR process [18]

1.1. The oxygen Carrier in the CLPOX Process

A key component of the CLPOX process is the selection of a suitable oxygen carrier with desirable properties such as: high reactivity, resistant to coke formation, resistant to attrition and sintering through a continuous cycle to cycle operation leading to an extended durability [19].

Some authors have studied several metals such as Fe, Ni, Cu, Co and Mn as oxygen carriers supported in different ceramics like α-Al_2O_3, γ-Al_2O_3, $MgAl_2O_4$, SiO_2, and Mg-ZrO_2 prepared through different techniques [20]. Zatar et al [21] found higher reactive particles composed by Fe, Mn, Ni and Cu supported on $MgAl_2O_4$ compared to those supported on SiO_2. Furthermore, Kale et al [18] reported that CuO happened to be a good oxygen carrier, since showed a complete conversion of ethanol withy easy regenerability.

CuO as oxygen carrier has been extensively studied due to its high reactivity, oxygen transport capacity and lack of thermodynamic limitations to completely oxidize a fuel [22]. While several supports have been successfully tested for CuO as oxygen carrier, Al_2O_3 has been the most often employed [23]. Furthermore, one of the advantages of the use of metals such as Cu and Ni is the fact that they are able to catalyze the SR nad POX reaction, while the mayor disadvantage of NiO resides in its propensity to produce carbon deposits. Therefore, a careful selection of the oxygen carrier is of paramount importance in this CLPOX process.

Several studies have determined the amount of hydrogen yield and carbon formation for the most thermodynamically viable oxygen carriers in CLPOX technology, and these include Fe_3O_4, Mn_2O_3, CoO, CuO and NiO [24]. Recent studies have reported that from most of metal oxides available NiO, CuO and CoO are the oxygen carriers that present the highest amount of O_2 (0.5 mols) per mol of metal [21-26]. Furthermore, they reported that the order from highest to lowest H_2 production was: $Fe_3O_4 > CoO > NiO = CuO > Mn_2O_3$. However, carbon formation increased in the order: $Mn_2O_3 > Fe_3O_4 > CoO > CuO = NiO$.

Therefore, a suitable metal oxide to be used in the present thermodynamic analysis can be either NiO or CuO or even a mixture of them.

Another important issue towards the selection of the oxygen carrier is its melting point. The melting point should be high enough to withstand the CLPOX reaction temperature process and to avoid sintering of the circulating particles. Rydén et al [26] found that Cu melting point was too low to withstand the high temperatures required by the CLPOX process, unless this is dispersed in suitable support. While, iron and Mn oxides are known to be hard to reduce and to produce significant amount of carbon compared to other oxides at the same conditions. Also, Ni in known to withstand high temperatures when used as a reforming catalyst supported in a ceramic material. Therefore, based on previous studies it is possible to select Cu and Ni or even a mixture of both to be used in the following proposed reaction system.

1.2. Chemical Looping Autothermal Ethanol Reforming with CO_2 Capture System

Studies in the field argue that even though steam can be added to the fuel (ethanol) to enhance the highly endothermic SR reaction, this could cause the SRE to dominate over the POX process causing a great heat demand in the reaction system. However, the introduction of the exothermic nature of the POX reaction through an oxygen carrier is intended to balance the heat demand to make this process autothermal in nature.

Nevertheless, one disadvantage of the use of Ni as an oxygen carrier is that its POX reaction with ethanol as a fuel is of endothermic nature. On the opposite for CuO this reaction is exothermic if a proper amount of oxides are provided:

$$C_2H_5OH + 3NiO \longrightarrow 3H_2 + 2CO_2 + 3Ni \qquad \Delta H^0 = +166.9 \text{ kJ/mol} \qquad (5)$$

$$C_2H_5OH + 3CuO \longrightarrow 3H_2 + 2CO_2 + 3Cu \qquad \Delta H^0 = -84.8 \text{ kJ/mol} \qquad (6)$$

while a complete list of possible involved reactions are reported elsewhere [27]

Furthermore, the introduction of a CO_2 absorbent in the system will presumably shift the equilibrium of the above POX reactions towards a higher H_2 production by:

$$C_2H_5OH + 3NiO + 2CaO \longrightarrow 3H_2 + 2CaCO_3 + 3Ni \qquad \Delta H^0 = -189.5 \text{ kJ/mol} \qquad (7)$$

$$C_2H_5OH + 3CuO + 2CaO \longrightarrow 3H_2 + 2CaCO_3 + 3Cu \qquad \Delta H^0 = -441.2 \text{ kJ/mol} \qquad (8)$$

These reactions are both exothermic and then combined with the endothermic nature of the ethanol reforming reaction (1) will result in the overall reaction system to eventually reach a thermoneutral state (autothermal operation) at suitable operation conditions. Therefore, the target is to generate hydrogen/Syngas in the fuel reactor by the combination of the POX, SER and CO_2 capture reactions through:

$$C_2H_5OH + NiO + CaO + H_2O \longrightarrow CO + 4H_2 + CaCO_3 + Ni \qquad \Delta H^0 = +34.1 \text{ kJ/mol} \quad (9)$$

$$C_2H_5OH + CuO + CaO + H_2O \longrightarrow CO + 4H_2 + CaCO_3 + Cu \qquad \Delta H^0 = -49.8 \text{ kJ/mol} \quad (10)$$
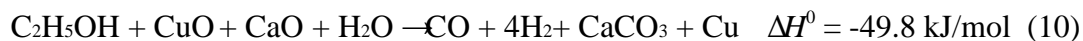
Even though, these reactions are endothermic or exothermic in nature, proper amounts of NiO and/or CuO would make these thermoneutral. Furthermore, regeneration of the oxygen carriers and CO_2 absorbent are to be performed at the air reactor, where the following reactions are expected to take place:

$$2Ni + 2CaCO_3 + O_2 = 2CO_2 + 2NiO + 2CaO \qquad \Delta H^0 = -123.1 \text{ kJ/mol} \qquad (11)$$

$$2Cu + 2CaCO_3 + O_2 = 2CO_2 + 2CuO + 2CaO \qquad \Delta H^0 = +44.8 \text{ kJ/mol} \qquad (12)$$

The amount of metal oxide (CuO or NiO) and/or CO_2 absorbent (CaO) in order to make this reaction system suitable to operate at the highest possible H_2/Syngas production and at thermoneutral conditions is not an obvious issue. Therefore, the aim of the present thermodynamic study is to explore possible ethanol chemical looping partial oxidation-steam reforming with CO_2 absorption (CLPOX-SR-CO_2A) to produce H_2/Syngas at autothermal and efficient conditions. This reactions system will make use of CuO and NiO as oxygen carrier materials, while CaO will be employed as a CO_2 absorbent.

2. Simulation Methodology: Thermodynamics Method

Thermodynamic calculations employed the Gibbs free energy minimization technique. In a reaction system where many simultaneous reactions take place, equilibrium calculations can be performed through the Gibbs energy minimization approach (also called the nonstoichiometric method). Details of this technique can be found elsewhere [28]. All calculations were performed using the equilibrium module of the HSC chemistry software for windows [29]. HSC calculates the equilibrium composition of all possible combination of reactions that are able to take place within the thermodynamic system. These equilibrium calculations make use of the equilibrium composition module of the HSC program that is based on the Gibbs free energy minimization technique. The GIBBS program of this module finds the most stable phase combination and seeks the phase compositions where the Gibbs free energy of the system reaches its minimum at a fixed mass balance, constant pressure and temperature. Within the ethanol CLPOX-SR-CO_2A system the gaseous species included were: ethanol, ethylene, ethane, acetone, acetaldehyde, acetic acid, C_2H_6O, CO, CH_4, CO_2, H_2, and H_2O, while solid species were: C, CaO, $CaCO_3$, Cu, CuO, Ni and NiO.

During the thermodynamic simulation work the reaction temperature was varied in the range of 100-1000 °C at 1 atm. H_2O/C_2H_5OH molar ratio was allowed to change from 3:1 to 6:1, carbonate to ethanol molar ratio ($CaCO_3/C_2H_5OH$) was varied from 1:1 to 2:1 while CuO/C_2H_5OH and NiO/C_2H_5OH molar ratios varied from 0.05:1 to 1.5:1 (all these values were determined according to the stoichiometric numbers from reactions 9 and 10). It is important to notice that all the ratios will be allowed to vary in order to find a thermoneutral (autothermal) point that favors the H_2/syngas production. Furthermore, the conditions here determined in the present thermodynamic analysis are based on theoretical considerations and these are to be taken as a guide to further experimental evaluation of the reaction system, since no heat and mass diffusional limitations as well as kinetics effects were taken into account for the conformation of the present thermodynamic analysis.

3. Results and Discussion

3.1 Thermodynamic Analysis

Table 1 presents results of the equilibrium molar content (H_2, CO, CO_2, CH_4 and C) for the steam reforming of ethanol (SRE) at the maximum hydrogen production and using H_2O/C_2H_6O molar ratios from 3 to 6. Here it can be seen that hydrogen production increased as the H_2O/C_2H_6O ratio also augmented, while the temperature for the maximum H_2 content decreased from 740°C at H_2O/C_2H_6O = 3 to 698 °C at H_2O/C_2H_6O = 6. Furthermore, CO_2 mols followed the same trend as H_2 content, while CO and CH_4 content decreased. This behavior is consistent with the promotion of the water gas shift (WGS, $CO + H_2O = CO_2 + H_2$) and the methane steam reforming (SMR, $CH_4 + 2H_2O = CO_2 + 4H_2$) reactions as temperature increased. It is important to address that no carbon formation is thermodynamically possible at the maximum H_2 production conditions. These results are in agreement with previous studies where higher H_2 yields resulted at molar feed ratios (H_2O/C_2H_6O) greater than 3 [30-32].

Table 1. Equilibrium molar content (H_2, CO, CO_2, CH_4 and C) at maximum hydrogen production and adiabatic conditions for the SRE reaction system.

Molar Feed			T °C	Max H_2 Production, Equilibrium Content, kmols					T_{adiab} °C	Adiabatic T Equilibrium Content, kmols				
H_2O/C_2H_5OH	NiO	CaO		H_2	CO	CO_2	CH_4	C		H_2	CO	CO_2	CH_4	C
3	0.0	0	740	4.47	1.37	0.580	0.0360	0.0000	338	0.3308	0.00267	0.58071	1.4166	0.000
4	0.0	0	740	4.71	1.22	0.770	0.0180	0.0000	298	0.2471	0.00087	0.56111	1.4380	0.000
5	0.0	0	705	4.88	1.00	0.968	0.0270	0.0000	272	0.1919	0.00035	0.54772	1.4519	0.000
6	0.0	0	698	5.03	1.10	0.879	0.0210	0.0000	254	0.1633	0.54068	0.00018	1.4591	0.000
0	0.8	0	900	2.86	1.59	0.049	0.0108	0.3520	343	0.2156	0.00105	0.16360	0.6563	1.179
0	0.9	0	900	2.84	1.63	0.063	0.0085	0.2960	325	0.1707	0.00063	0.16563	0.6306	1.203
0	1.0	0	900	2.81	1.66	0.080	0.0066	0.2489	298	0.1165	0.00028	0.16271	0.6046	1.232
0	1.1	0	900	2.77	1.68	0.100	0.0051	0.2109	281	0.0880	0.00015	0.16524	0.5713	1.263
0	1.2	0	900	2.73	1.69	0.124	0.0040	0.1805	255	0.0557	0.00006	0.16269	0.5349	1.302
0	1.3	0	900	2.68	1.69	0.150	0.0032	0.1565	237	0.0398	0.00003	0.49569	0.1656	1.339
0	1.4	0	900	2.63	1.68	0.178	0.0025	0.1374	210	0.0230	0.00001	0.16289	0.4514	1.386
0	1.5	0	900	2.58	1.67	0.207	0.0020	0.1219	188	0.0125	0.00000	0.15972	0.4035	1.437

Also in Table 1 results for equilibrium SRE at the adiabatic temperature (T_{adiab}, $\Delta H \approx 0$) are shown. As stated earlier it is possible for the SRE reaction system to reach autothermal conditions. Here, it can be seen that at all adiabatic SRE conditions temperatures and H_2 content are low, consequently CO_2 and CH_4 content are high as the reverse WGS and SMR are favored with no carbon formation. This result was expected, since the nature of the SRE reaction (1) is endothermic.

Furthermore, in Table 1 the equilibrium content at the maximum H_2 production temperature for the partial oxidation of ethanol using NiO as an oxygen source is presented. Here, the NiO/C_2H_6O molar ratio was varied from 0.8-1.5. Results indicate that the maximum H_2 production was found at the end upper temperature limit of 900 °C, with only an average H_2 content of 2.74 kmols disregarding the amount of oxygen content on NiO in the reaction system. In fact, as the NiO/C_2H_6O molar ration increased, there is a slight reduction of the amount of H_2 produced at 900 °C. This is consistent with the partial oxidation of ethanol to syngas and the Boudouard reactions:

$$C_2H_5OH + NiO \longrightarrow 3H_2 + 2CO + Ni \qquad \Delta H^0 = +253.4 \text{ kJ/mol} \qquad (13)$$

$$2CO \rightarrow CO_2 + C \qquad\qquad \Delta H^0 = -175.81 \text{ kJ/mol} \qquad\qquad (14)$$

at these conditions, the concentration of CO_2 is small and there is a large amount of C being formed. Even though, there exists an excess of NiO in the reaction system the formation of C is still present, this in contrast with the SRE system, where the presence of steam prevents the formation of carbon deposits. Furthermore, in Table 1 the equilibrium content at adiabatic conditions (T_{adiab}, $\Delta H \approx 0$) is shown for the ethanol POX with NiO. At these adiabatic conditions the maximum H_2 content was of 0.216 kmols at 343 °C and $NiO/C_2H_5OH = 0.8$. Greater amounts of NiO will generate lower adiabatic temperatures and H_2 production, while greater amounts of carbon and carbon dioxide (through the Boudouard reaction) are present. This behavior is expected, since POX reactions with NiO (5 and 13) are both endothermic in nature.

Based on the results described above it is evident the need an additional reaction in order to balance out the SRE and POX reaction (both endothermic) with another highly exothermic reaction. This reaction is the CO_2 absorption with CaO:

$$CaO + CO_2 \rightarrow CaCO_3 \qquad\qquad \Delta H^0 = -178.17 \text{ kJ/mol} \qquad\qquad (15)$$

This reaction will not only alleviate the heat needed for the reaction system for a possible autothermal operation, but will reduce the CO_2 content in the gas product by modifying the thermodynamics of both SER and POX reactions towards a greater H_2 production.

Table 2 presents results of the equilibrium molar content (H_2, CO, CO_2, CH_4 and C) for the combination of SRE, POX and CO_2 absorption (reaction 9) of ethanol at the maximum hydrogen production using $NiO/C_2H_5OH = 1$ and varying the H_2O/C_2H_5OH ratio from 3 to 6.

The CaO feed was kept at 2 kmols to insure the complete CO_2 absorption in the reaction system. Here, it can be observed that the maximum H_2 content occurred in a very narrow temperature range from 625 to 679 °C at H_2O/C_2H_5OH ratios of 6 and 3, respectively. In this region syngas production (CO + H_2) is favored as reaction (13) is thermodynamically feasible. Also, the CO_2 content is low due to CaO carbonation reaction (15) being promoted, shifting the equilibrium towards greater H_2 production in reaction (9). This carbonation reaction did not only had an effect on the H_2 production, but also on reduction of carbon formation as can be seen in Table 2.

.   Also, in Table 2, the equilibrium content at adiabatic conditions (T_{adiab}, $\Delta H \approx 0$) is shown for the combined ethanol of SRE, POX and CO_2 absorption reaction system at $NiO/C_2H_5OH = 1$ and H_2O/C_2H_6O from 3 to 6. At these conditions, the adiabatic temperature varied from 466 to 382 °C at H_2O/C_2H_6O ratios of 3 and 6, respectively. Hydrogen production at adiabatic conditions do not differ significantly with respect to the values found at the higher temperatures of the maximum hydrogen production. This can be explained in term that at the adiabatic temperatures (382-466 °C) the carbonation reaction is even more thermodynamically favored and this being reflected in very small CO_2 concentrations as seen in Table 2 for these conditions.

Table 2. Equilibrium molar content (H_2, CO, CO_2, CH_4 and C) at maximum H_2 production and adiabatic conditions for the SRE, CLPOX and CO_2 capture combined process reaction system using NiO as oxygen carrier.

Molar Feed			T °C	Max H₂ Production, Equilibrium Content, kmols					T_{adiab} °C	Adiabatic T Equilibrium Content, kmols				
H_2O/C_2H_5OH	NiO	CaO		H_2	CO	CO_2	CH_4	C		H_2	CO	CO_2	CH_4	C
3.0	1.00	2	679	4.19	0.34	0.241	0.0520	0.1306	466	3.85	0.00054	0.00145	0.27390	0.02795
3.5	1.00	2	670	4.33	0.41	0.328	0.0450	0.1000	449	4.02	0.00026	0.00097	0.23826	0.01718
4.0	1.00	2	661	4.45	0.24	0.255	0.0400	0.0780	431	4.15	0.00012	0.00060	0.20908	0.01067
4.5	1.00	2	652	4.54	0.20	0.255	0.0350	0.0620	418	4.25	0.00008	0.00052	0.18332	0.00793
5.0	1.00	2	643	4.61	0.17	0.250	0.0316	0.0500	405	4.34	0.00003	0.00029	0.16389	0.00497
5.5	1.00	2	634	4.67	0.14	0.243	0.0280	0.0410	391	4.41	0.00001	0.00015	0.14757	0.00309
6.0	1.00	2	625	4.72	0.11	0.233	0.0263	0.0350	382	4.47	0.00001	0.00012	0.13280	0.00233
3.0	0.05	2	732	4.78	0.91	0.289	0.0597	0.0122	502	4.06	0.00236	0.00288	0.47066	0.00404
3.0	0.10	2	732	4.75	0.89	0.295	0.0553	0.0229	502	4.06	0.00237	0.00297	0.45625	0.00795
3.0	0.15	2	723	4.72	0.81	0.282	0.0637	0.0365	502	4.06	0.00237	0.00306	0.44224	0.01163
3.0	0.25	2	723	4.65	0.77	0.292	0.0550	0.0525	493	4.04	0.00163	0.00239	0.41920	0.01578
3.0	0.50	2	705	4.50	0.51	0.274	0.0580	0.0930	484	4.00	0.00113	0.00204	0.36352	0.02384
3.0	1.00	2	679	4.19	0.34	0.241	0.0520	0.1306	466	3.85	0.00054	0.00145	0.27390	0.02795
3.0	1.50	2	661	3.87	0.22	0.222	0.0388	0.1311	444	3.63	0.00025	0.00101	0.20475	0.02507
4.0	0.05	2	697	5.13	0.56	0.303	0.0637	0.0076	467	4.58	0.00058	0.00144	0.34296	0.00137
4.0	0.10	2	687	5.09	0.49	0.283	0.0721	0.0161	467	4.56	0.00059	0.00148	0.33377	0.00276
4.0	0.15	2	688	5.06	0.48	0.286	0.0675	0.0229	458	4.54	0.00039	0.00108	0.32690	0.00348
4.0	0.25	2	687	4.99	0.46	0.292	0.0593	0.0342	458	4.50	0.00039	0.00115	0.30967	0.00562
4.0	0.50	2	679	4.81	0.37	0.281	0.0520	0.0565	449	4.40	0.00026	0.00093	0.27211	0.00876
4.0	1.50	2	643	4.07	0.15	0.225	0.0301	0.0819	413	3.85	0.00005	0.00038	0.15867	0.00974
5.0	0.05	2	670	5.37	0.35	0.295	0.0572	0.0047	431	4.90	0.00012	0.00056	0.26259	0.00051
5.0	0.10	2	670	5.33	0.34	0.297	0.0539	0.0092	431	4.88	0.00012	0.00057	0.25614	0.00105
5.0	0.15	2	661	5.29	0.29	0.273	0.0603	0.0142	426	4.85	0.00012	0.00059	0.24981	0.00156
5.0	0.25	2	661	5.21	0.28	0.277	0.0537	0.0217	422	4.79	0.00008	0.00043	0.23909	0.00214
5.0	0.50	2	652	5.01	0.23	0.260	0.0475	0.0368	413	4.65	0.00005	0.00033	0.21198	0.00337
5.0	1.50	2	625	4.20	0.11	0.214	0.0242	0.0546	387	3.99	0.00001	0.00017	0.12576	0.00454
6.0	0.05	2	652	5.53	0.24	0.289	0.0454	0.0029	396	5.12	0.00002	0.00017	0.20943	0.00019
6.0	0.10	2	652	5.49	0.23	0.290	0.0430	0.0059	396	5.08	0.00002	0.00018	0.20459	0.00040
6.0	0.15	2	652	5.44	0.23	0.291	0.0408	0.0087	396	5.05	0.00002	0.00018	0.19984	0.00060
6.0	0.25	2	643	5.36	0.19	0.267	0.0430	0.0142	400	4.99	0.00002	0.00019	0.19058	0.00099
6.0	0.50	2	625	5.14	0.21	0.301	0.0280	0.0224	396	4.83	0.00002	0.00022	0.16881	0.00190
6.0	1.50	2	617	4.28	0.08	0.218	0.0176	0.0375	369	4.09	0.00001	0.00010	0.10195	0.00259

Also, CO and C content are reduced at adiabatic conditions. All these features make a very attractive operating conditions for reaction (9). However, kinetic and catalytic limitations have been reported for the steam reforming of ethanol at temperatures below 500° C as reported elsewhere [31, 32]. Therefore, even though favorable adiabatic conditions exist at $NiO/C_2H_5OH = 1$ and H_2O/C_2H_5OH from 3 to 6, it is required to find (at least from a thermodynamic point of view) conditions for adiabatic temperatures greater than 500 °C.

Furthermore, Table 2 presents results for the SRE, POX and CO_2 absorption combined system fixing the H_2O/C_2H_5OH ratio at 3, 4, 5 and 6, while varying the NiO/C_2H_5OH ratio from 0.05 to 1.5, while keeping the $CaO/C_2H_6O = 2$.

Generally, from results of Table 2, it can be observed that the maximum H_2 production, occurred at $NiO/C_2H_6O < 1$ and this is increased as the H_2O/C_2H_6O also grew. More than 5 kmols of hydrogen are produced at $H_2O/C_2H_6O \geq 4$ and at temperatures between 620 and 700 °C. Even though at all these conditions there exist some carbon formation and this is relatively small with respect to other species. It is important to underline that selected conditions of the present study were chosen in order to minimize the carbon formation, but the combination of adiabatic conditions and high H_2 production resulted in only marginal C formation. Moreover, due to the configuration of the reaction process, the carbon deposited in the fuel reactor and ultimately over the catalyst, will be adequately removed in the air reactor (regenerator reactor) where the reduced Me is to be reoxidized back to MeO (see

Figure 1). This operation mode, in which deposited carbon is removed by another oxidizing reactor is well documented in the commercial FFC catalytic reactors [33] and in the CALCOR and Catforming commercial processes for ethanol dry reforming [34, 35]. However, kinetic may play a significant role at these reaction conditions, since there are some studies that report the kinetic propensity of Ni to form carbon deposits [36].

Table 2 additionally presents adiabatic equilibrium conditions for the combined SRE, POX and CO_2 absorption reaction system. Most favorable reactions conditions were encountered at $H_2O/C_2H_5OH = 3$ and NiO/C_2H_5OH ratios in the range of 0.05-0.25, where the adiabatic temperature is equal or greater than 500 °C. At these conditions there is a reasonable high concentration of H_2 at equilibrium with respect to other gaseous species and a relatively small amount of carbon formation, with the exception of CH_4, which is the other more concentrated specie in the gas product. However, experimental findings have concluded that at SRE of ethanol combined with CO_2 absorption reaction system conditions, methane formation is kinetically limited as a recent study have reported [37]. It is important to point out that these favorable reaction conditions are the product of the combination of the exothermic carbonation reaction and its influence over the thermodynamic equilibrium over the POX and SRE endothermic reactions.

Moreover, Table 3 presents results of the equilibrium molar content (H_2, CO, CO_2, CH_4 and C) for the combination of SRE, POX and CO_2 absorption (reaction 10) of ethanol at the maximum hydrogen production using $CuO/C_2H_5OH = 1$ and varying the H_2O/C_2H_5OH ratio from 3 to 6. Again, here, CaO feed was kept at 2 kmols to insure the complete CO_2 absorption in the reaction system. From this table it can be observed that the maximum H_2 content occurred, similarly as in the case of with NiO, in a very narrow temperature range from 625 to 688 °C at H_2O/C_2H_5OH ratios of 6 and 3, respectively. In this region Syngas production (CO + H_2) is favored as the following reaction is thermodynamically favored:

$$C_2H_5OH + CuO \longrightarrow 3H_2 + 2CO + Cu \qquad \Delta H^0_{298} = +169.5 \text{ kJ/mol} \qquad (16)$$

as well as CO_2 is produced as the exothermic reaction (6) is favored, while methane and carbon content are rather small in this region. Also in this Table, it is important to indicate that adiabatic temperatures present values greater than 500 °C (519-590). However, at these conditions CO_2 and CH_4 content are rather high as Solunke and Vesser have reported in their thermodynamic calculations [38]. This feature can create an additional purification step for H_2 and or syngas.

Table 3 additionally presents maximum H_2 production equilibrium conditions for the combined SRE, POX and CO_2 absorption reaction fixing the H_2O/C_2H_5OH ratio at 3, 4, 5 and 6, while varying the CuO/C_2H_5OH ratio from 0.05 to 1.5, and keeping the $CaO/C_2H_5OH = 2$. From results of Table 3, it can be observed that the maximum H_2 production, occurred at $CuO/C_2H_5OH < 1$ and this is increased as the H_2O/C_2H_5OH also grew. More than 5 kmols of hydrogen are produced at $H_2O/C_2H_5OH \geq 4$ and at temperatures between 634 and 697 °C. Even though at all these conditions there exist some carbon formation and this is relatively small with respect to other species.

Also, Table 3 shows adiabatic equilibrium conditions for the combined SRE, POX and CO_2 absorption reaction system. Most favorable reactions conditions; $T \geq 500$ °C and small carbon formation, $C \leq 0.1$ kmols, were encountered at several regions: i) at $H_2O/C_2H_5OH = 3$ and all CuO/C_2H_5OH ratios (0.05-1.5), ii) at $H_2O/C_2H_6O = 4$ and CuO/C_2H_5OH ratios of

0.25-1.5, and finally iii) at $H_2O/C_2H_5OH = 5$ and 6 with a CuO/C_2H_5OH ratio of 1.5. At all these adiabatic conditions, hydrogen production higher than 4 kmols at equilibrium occurred at all H_2O/C_2H_5OH ratios, with the exemption of $H_2O/C_2H_5OH = 3$ and $CuO/C_2H_5OH = 1.5$, while maximum H_2 production at adiabatic conditions was found at $H_2O/C_2H_5OH = 4$, $CuO/C_2H_5OH = 0.5$ and $T_{adiab} = 529$ °C, where 4.48 kmols of H_2 are produced at equilibrium. At this condition, very small amount of carbon oxides are generated as well as carbon formation (C = 0.032 kmols). Again, these favorable reaction conditions are the product of the combination of the exothermic carbonation reaction and its influence over the thermodynamic equilibrium over the POX and SRE endothermic reactions.

Furthermore, the production of hydrogen and equilibrium molar content of CO, CO_2 and C at a temperature range of 100-900 °C and CuO/C_2H_5OH molar ratios from 0.05 to 1.5 (CaO feed of 2 kmols) are presented in Figure 2. This Figure shows the equilibrium content for H_2 and CO while Figure 3 for CO_2 and CH_4.

Table 3. Equilibrium molar content (H_2, CO, CO_2, CH_4 and C) at maximum H_2 production and adiabatic conditions for the SRE, CLPOX and CO_2 capture combined process reaction system using CuO as oxygen carrier.

Molar Feed			T °C	Max H₂ Production, Equilibrium Content, kmols					T_adiab °C	Adiabatic T Equilibrium Content, kmols				
H₂O/C₂H₅OH	CuO	CaO		H₂	CO	CO₂	CH₄	C		H₂	CO	CO₂	CH₄	C
3.0	1.00	2	688	4.19	0.39	0.265	0.0440	0.1233	590	4.04	0.05301	0.05930	0.16261	0.12894
3.5	1.00	2	670	4.33	0.29	0.251	0.0453	0.1001	581	4.19	0.04363	0.06120	0.14205	0.09711
4.0	1.00	2	661	4.44	0.24	0.255	0.0397	0.0783	564	4.30	0.02728	0.05010	0.13350	0.07022
4.5	1.00	2	652	4.53	0.20	0.255	0.0352	0.0625	555	4.40	0.02175	0.04866	0.11819	0.05499
5.0	1.00	2	643	4.61	0.17	0.250	0.0315	0.0508	537	4.46	0.01287	0.03691	0.11238	0.04057
5.5	1.00	2	634	4.66	0.14	0.243	0.0285	0.0419	528	4.52	0.00997	0.03412	0.10151	0.03263
6.0	1.00	2	625	4.71	0.11	0.233	0.0261	0.0351	519	4.57	0.00765	0.03095	0.09257	0.02652
3.0	0.05	2	732	4.78	0.91	0.289	0.0596	0.0126	511	4.07	0.00343	0.00390	0.46740	0.00486
3.0	0.10	2	723	4.75	0.83	0.278	0.0686	0.0267	520	4.08	0.00493	0.00540	0.44889	0.01092
3.0	0.15	2	723	4.72	0.81	0.283	0.0635	0.0369	528	4.09	0.00702	0.00740	0.42936	0.01828
3.0	0.25	2	723	4.65	0.77	0.293	0.0549	0.0529	537	4.10	0.00986	0.01032	0.39397	0.03251
3.0	0.50	2	706	4.50	0.58	0.275	0.0579	0.0934	555	4.10	0.01855	0.01977	0.30985	0.06879
3.0	1.00	2	688	4.19	0.39	0.265	0.0440	0.1233	590	4.04	0.05301	0.05930	0.16261	0.12894
3.0	1.50	2	661	3.86	0.22	0.222	0.0386	0.1310	617	3.83	0.09328	0.11695	0.07380	0.13998
4.0	0.05	2	697	5.13	0.55	0.303	0.0635	0.0080	467	4.58	0.00058	0.00144	0.34252	0.00144
4.0	0.10	2	688	5.09	0.49	0.283	0.0718	0.0165	476	4.57	0.00088	0.00208	0.33115	0.00331
4.0	0.15	2	688	5.06	0.48	0.286	0.0672	0.0232	485	4.56	0.00132	0.00296	0.31950	0.00568
4.0	0.25	2	688	4.98	0.46	0.292	0.0591	0.0345	502	4.54	0.00288	0.00585	0.29500	0.01221
4.0	0.50	2	679	4.81	0.37	0.282	0.0518	0.0567	529	4.48	0.00840	0.01569	0.23667	0.03215
4.0	1.50	2	644	4.06	0.15	0.225	0.0299	0.0818	599	4.04	0.06354	0.11775	0.05716	0.08616
5.0	0.05	2	670	5.37	0.35	0.295	0.0569	0.0050	440	4.91	0.00019	0.00081	0.26065	0.00065
5.0	0.10	2	670	5.33	0.34	0.297	0.0537	0.0096	449	4.89	0.00030	0.00120	0.25248	0.00152
5.0	0.15	2	661	5.29	0.29	0.273	0.0600	0.0145	458	4.87	0.00046	0.00176	0.24420	0.00265
5.0	0.25	2	661	5.21	0.28	0.277	0.0534	0.0220	466	4.82	0.00071	0.00261	0.22946	0.00502
5.0	0.50	2	652	5.01	0.23	0.260	0.0472	0.0370	493	4.71	0.00237	0.00777	0.19070	0.01437
5.0	1.50	2	625	4.19	0.11	0.214	0.0240	0.0545	572	4.15	0.03361	0.09314	0.05117	0.05549
6.0	0.05	2	652	5.52	0.24	0.289	0.0451	0.0032	405	5.12	0.00003	0.00026	0.20792	0.00025
6.0	0.10	2	652	5.48	0.23	0.290	0.0428	0.0062	413	5.09	0.00006	0.00040	0.20187	0.00061
6.0	0.15	2	644	5.44	0.20	0.265	0.0476	0.0094	422	5.06	0.00009	0.00060	0.19580	0.00108
6.0	0.25	2	644	5.36	0.19	0.267	0.0428	0.0144	440	5.01	0.00023	0.00135	0.18351	0.00249
6.0	0.50	2	634	5.14	0.16	0.247	0.0383	0.0247	467	4.86	0.00085	0.00436	0.15527	0.00755
6.0	1.50	2	617	4.27	0.08	0.218	0.0174	0.0375	555	4.23	0.02133	0.08099	0.04302	0.03822
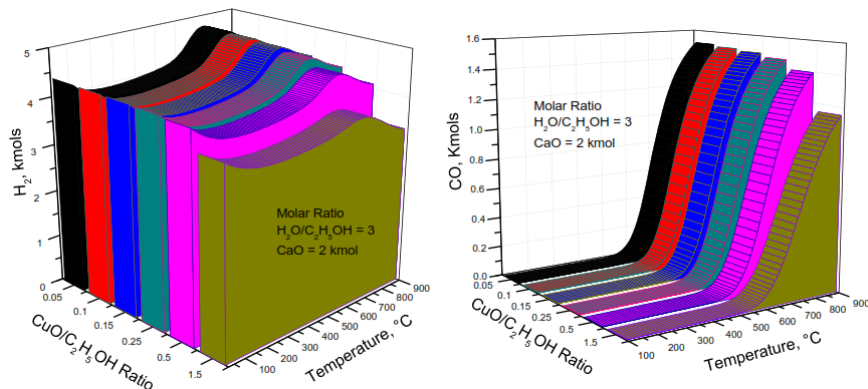
Fig 2. Equilibrium content of H_2 and CO for the SRE, CLPOX and CO_2 capture combined process

In Figure 2 it is evident that H_2 mols at equilibrium are always greater than 4 kmols and this is due to the shift in equilibrium towards a greater hydrogen production in reaction (10). A maximum H_2 can be found at a temperature range from 661-732 °C as also can be seen in results from Table 3. While in Figure 2, CO concentration is kept low for the temperature range from 100-550 °C and this is due to the combination of the water gas shift and the CO_2 carbonation reactions, thus producing more H_2 and CO_2 (through WGS), which is finally trapped in $CaCO_3$. Greater values of 550 °C will hamper the ability of CaO to capture CO_2, since greater carbon dioxide partial pressures will shift the equilibrium of reaction (15) towards decarbonation of $CaCO_3$. This behavior is reflected in Figure 3 where the CO_2 content is shown to be negligible in the temperature range from 100-550 °C at all CuO/C_2H_5OH molar ratios. Meanwhile, CH_4 content (Figure 3) results in values less than 0.5 kmols at a temperature range from 100-650 °C, where the endothermic steam methane reaction takes over the reaction system to produce more hydrogen and CO_2 at higher temperatures.
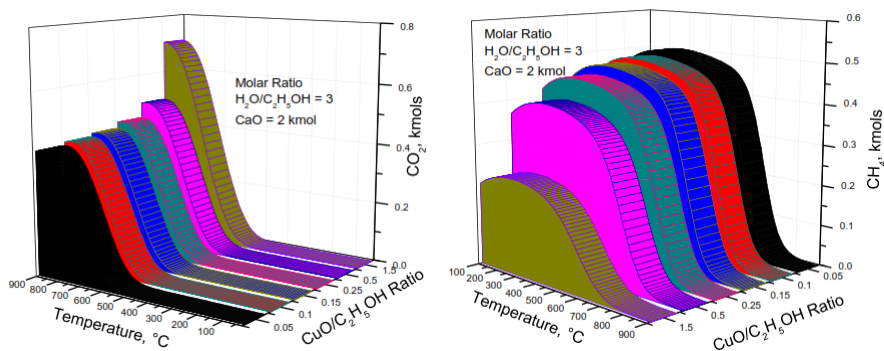
Fig 3. Equilibrium content of CO_2 and CH_4 for the SRE, CLPOX and CO_2 capture combined process

Finally, Figure 4 presents the carbon content at equilibrium for the reaction system. In this plot it is clear that in a temperature range 100 – 500 °C carbon formation is almost negligible at all CuO/C_2H_6O molar ratios. Here it can be seen that as CuO/C_2H_5OH increases carbon formation will grow. However, the carbon formed at equilibrium in Figure 4 is always less than 0.15 kmols at all presented conditions. All the previous results are in agreement with thermodynamic analysis data reported by Wang and Cao [27] for similar reaction conditions.
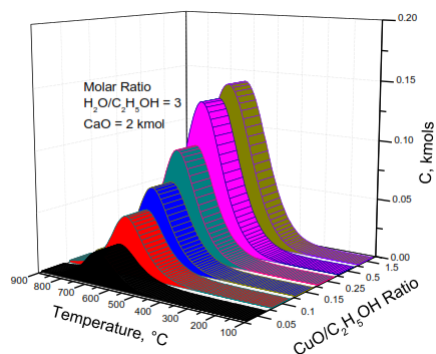
Fig 4. Equilibrium content of C for the SRE, CLPOX and CO_2 capture combined process

Figure 5 presents two plots for the adiabatic temperature (°C) and the equilibrium molar content at $H_2O/C_2H_5OH = 3$ and the corresponding adiabatic temperature as a function of NiO/C_2H_5OH (Figure 5) and CuO/C_2H_5OH (Figure 5). In this it is evident that for the NiO/C_2H_5OH range of 0.05-0.15 adiabatic temperatures are ≥ 500 °C, whereas higher molar ratios will lead to lower adiabatic temperatures. At this condition (T ≥ 500 °C) it is clear that values of H_2 content are ≥ 4 kmols. Lower adiabatic temperatures and H_2 content will arise when $NiO/C_2H_5OH > 0.15$. This attractive operating adiabatic range (T ≥ 500 °C and $NiO/C_2H_5OH = 0.05$-0.15) can be explained in terms of the combined effects of the highly endothermic nature of the SRE and POX reactions and the counter effect achieved by the highly exothermic CaO carbonation reaction. This effect is even clearer, since at this region CO_2 concentrations are almost negligible in Figure 5.
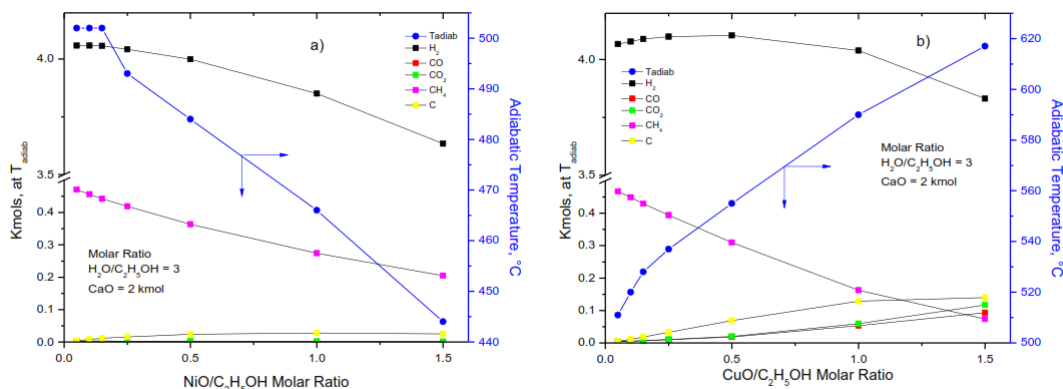
Fig 5. Adiabatic temperature and species equilibrium content as a function of metal oxide and steam content.

Moreover, Figure 5 shows the adiabatic temperature (°C) and the equilibrium molar content at $H_2O/C_2H_5OH = 3$ and the corresponding adiabatic temperature as a function of CuO/C_2H_5OH. In this plot it is interesting to realize that as the NiO/C_2H_5OH increases, the adiabatic temperature also rises. This can be explained in terms of the combined nature of reactions (6) and (8), which both are exothermic in nature. This is the reason why the NiO adiabatic temperature curve from Figure 5 (a) presents an opposite trend with respect to the use of CuO as oxygen carrier in Figure 5 (b). Furthermore, it is important to mention that all adiabatic temperature values presented in Figure 5 (b) are greater than 500 °C and that in a CuO/C_2H_5OH range of 0.05-0.15 hydrogen production is always greater than 4 kmols at equilibrium.

4. Conclusion

In the present work a thermodynamic analysis was performed to explore reaction conditions at equilibrium for a high syngas-H_2 production and adiabatic temperatures, under the combined ethanol steam reforming (SRE) , chemical looping partial oxidation (CLPOX) and CO_2 solid absorption reaction system. SRE studied conditions were in a range of $H_2O/C_2H_5OH = 3$ to 6 molar ratio, CLPOX employed NiO and CuO as oxygen carriers and varied from $MeO/C_2H_5OH = 0.05$ to 1.5 molar ratio, while 1 kmols of CaO were used for CO_2 Capture in the reaction system in temperature range of 100-900 °C at atmospheric conditions. Results indicate that for NiO the maximum H_2 content occurred in a T range of 625 to 679 °C at H_2O/C_2H_5OH ratios of 6 and 3, respectively and most favorable reactions conditions (T $\geq$ 500 °C and small carbon formation, C $\leq$ 0.1 kmols) were encountered at $H_2O/C_2H_5OH = 3$ and NiO/C_2H_5OH ratios in the range of 0.05-0.25, where the adiabatic temperature is equal or greater than 500 °C. At these conditions there is a reasonable high concentration of H_2 at equilibrium with respect to other gaseous species and a relatively small amount of carbon formation. While, for CuO as oxygen carrier, the maximum H_2 content occurred, similarly as in the case of with NiO, in a T range from 625 to 688 °C at H_2O/C_2H_6O ratios of 6 and 3, respectively. Alternatively, Most favorable adiabatic reactions conditions with CuO were encountered at several regions: i) at $H_2O/C_2H_6O = 3$ and all CuO/C_2H_5OH ratios (0.05-1.5), ii) at $H_2O/C_2H_5OH = 4$ and CuO/C_2H_5OH ratios of 0.25-1.5, and finally iii) at $H_2O/C_2H_5OH = 5$ and 6 with a CuO/C_2H_5OH ratio of 1.5. Finally, it was concluded that these favorable reaction conditions are the product of the combination of the exothermic carbonation reaction and its influence over the thermodynamic equilibrium over the POX and SRE endothermic reactions.

References

[1] Dou B. L., Song Y.C., Wang C., Chen H.S., Xu Y.J., Hydrogen production from catalytic steam reforming of biodiesel byproduct glycerol: issues and challenges. Renewable Sustainable Energy Rev, 30 (2014), pp. 950–960.
[2] Mazloomi K., Gomes C. Hydrogen as an energy carrier: prospects and challenges. Renewable Sustainable Energy Rev, 16 (2012), pp. 3024–3033.
[3] Chaubey R., Sahu S., James O.O., Maity S. A review on development of industrial processes and emerging techniques for production of hydrogen from renewable and sustainable sources. Renewable Sustainable Energy Rev, 23 (2013), pp. 443–462.

[4] Taboada E., Angurell I., Llorca J. Dynamic photocatalytic hydrogen production from ethanol–water mixtures in an optical fiber honeycomb reactor loaded with Au/TiO$_2$. J Catal, 309 (2014), pp. 460–467.

[5] Ni M, Leung MKH, Leung DYC, Sumathy K. A review and recent developments in photocatalytic water-splitting using TiO$_2$ for hydrogen production. Renewable Sustainable Energy Rev, 11 (2007), pp. 401–425.

[6] Marone A., Izzo G., Mentuccia L., Massini G., Paganin P., Rosa S., Varrone C., Signorini A. Vegetable waste as substrate and source of suitable microflora for bio-hydrogen production. Renewable Energy, 68 (2014), pp. 6–13.

[7] Faria E.C., Neto R.C.R., Colman R.C., Noronha F.B. Hydrogen production through CO2 reforming of methane over Ni/CeZrO$_2$/Al2O$_3$ catalysts. Catal Today, 228 (2014), pp. 138–144.

[8] Ni M., Leung D.Y.C., Leung M.K.H., Sumathy K. An overview of hydrogen production from biomass. Fuel Process Technol, 87 (2006), pp. 461–472.

[9] Augusto B.L., Costa L.O.O., Noronha F.B., Colman R.C., Mattos L.V. Ethanol reforming over Ni/CeGd catalysts with low Ni content. Int J Hydrogen Energy, 37 (2012), pp. 12258–12270.

[10] Li J., Yu H., Yang G., Peng F., Xie D., Wang H. Steam reforming of oxygenate fuels for hydrogen production: a thermodynamic study. Energy Fuels, 25 (2011), pp. 2643–2650.

[11] Díaz Alvarado F., Gracia F. Steam reforming of ethanol for hydrogen production: thermodynamic analysis including different carbon deposits representation. Chem Eng J, 165 (2010), pp. 649–657.

[12] Guil-López R., Navarro R.M., Peña M.A., Fierro J.L.G. Hydrogen production by oxidative ethanol reforming on Co, Ni and Cu ex-hydrotalcite catalysts. Int J Hydrogen Energy, 36 (2011), pp. 1512–1523.

[13] Kugai J., Subramani V., Song C., Engelhard M.H., Chin Y.H. Effects of nanocrystalline CeO$_2$ supports on the properties and performance of Ni–Rh bimetallic catalyst for oxidative steam reforming of ethanol. J Catal, 238 (2006), pp. 430–440.

[14] Ramírez de la Piscina P., Homs N. Use of biofuels to produce hydrogen (reformation processes). Chem Soc Rev, 37 (2008), pp. 2459–2467.

[15] Silva A.M., Costa L.O.O., Souza K.R., Mattos L.V., Noronha F.B. The effect of space time on Co/CeO2 catalyst deactivation during oxidative steam reforming of ethanol. Catal Commun, 11 (2010), pp. 736–74.

[16] Nishiguchi T., Matsumoto T., Kanai H., Utani K., Matsumura Y., Shen W. J., Imamura S. Appl Catal A-Gen, 2005, 279(1-2): 273.

[17] Mattisson T., Lyngfelt A. Applications of chemical looping combustion with capture of CO$_2$. In: Proc. 2nd Nordic Minisymposium on Carbon Dioxide Capture and Storage. Göteborg, Sweden; 2001.

[18] Kale G.R., Kulkarni B.D., Bharadwaj K.V. Chemical looping reforming of ethanol for syngas generation: a theoretical investigation. International Journal Energy Research 2013; 37:645–656.

[19] Adanez J., Abad A., Garcia-Labiano F., Gayan P., de Diego L.F. Progress in chemical-looping combustion and reforming technologies. Progress in Energy and Combustion Science 2012; 38:215–82.

[20] Ortiz M., Abad A., de Diego L.F., García-Labiano F., Gayán P., Adánez J. Optimization of hydrogen production by chemical-looping auto-thermal reforming working with Ni-based oxygen-carriers. International Journal of Hydrogen Energy 2011; 36:9663–72.

[21] Zafar Q., Mattisson T., Gevert B. Redox investigation of some oxides of transition-state metals Ni, Cu, Fe, and Mn supported on SiO2 and MgAl$_2$O$_4$. Energy and Fuels 2006; 20:34–44.

[22] Arjmand M., Azad A.M., Leion H., Lyngfelt A., Mattisson T. Prospects of Al$_2$O$_3$ and MgAl$_2$O$_4$-supported CuO oxygen carriers in chemical-looping combustion (CLC) and chemical-looping with oxygen uncoupling (CLOU). Energy and Fuels 2011; 25:5493–5502.

[23] de Diego L.F., García-Labiano F, Gayán P, Celaya J, Palacios J.M., Adánez J. Operation of a 10 kWth chemical-looping combustor during 200 h with a CuO/Al$_2$O$_3$ oxygen carrier. Fuel 2007; 86:1036–1045.

[24] Kale G.R., Kulkarni B.D., Bharadwaj K.V. Chemical looping reforming of ethanol for syngas generation: A theoretical investigation. International Journal of Energy Research 2013, Volume 37, Issue 6, pages 645–656.

[25] Comas J., Laborde M., Amadeo N. Thermodynamic analysis of hydrogen production from ethanol using CaO as a CO$_2$ sorbent. Journal of Power Sources 2004; 138:61–67.

[26] Rydén M., Lyngfelt A.,Mattisson T. Synthesis gas generation by chemical-looping reforming in a continuously operating laboratory reactor. Fuel 2006; 85:1631–1641.

[27] Wang W. Cao Y. A combined thermodynamic and experimental study on chemical-looping ethanol reforming with carbon dioxide capture for hydrogen generation. International Journal of Energy Research Int. J. Energy Res. 2013; 37:25–34.

[28] Collins-Martínez V. Escobedo Bretado M., Meléndez Zaragoza M., Salinas Gutiérrez J., López Ortiz A. Absorption enhanced reforming of light alcohols (methanol and ethanol) for the production of hydrogen: Thermodynamic modeling, Int J Hydrogen Energy 2013; 38:12539–553.

[29] Roine A. Chemical reaction and equilibrium software with extensive thermo-chemical database. Outokumpu HSC 6.0 Chemistry for windows; 2010.

[30] Collins-Martinez V., Escobedo Bretado M., Meléndez Zaragoza M., Salinas Gutiérrez J., López Ortiz A. Absorption enhanced reforming of light alcohols (methanol and ethanol) for the production of hydrogen: thermodynamic modeling. Int J Hydrogen Energy 2013; 28:12539-53.

[31] Fatsikostas A.N., Verykios X.E. Reaction network of steam reforming of ethanol over Ni-based catalysts. J Catal 2004; 225:439-52.

[32] Frusteri F., Freni S., Chiodo V., Spadaro L., Di Blasi O., Bonura G.. Cavallaro, steam and auto-thermal reforming of bio-ethanol over MgO and CeO2eNi supported catalysts. Int J Hydrogen Energy 2006; 31(15):2193-9.

[33] Sugungun M.M., Kolesnikov I.M., Vinogradov V.M., Kolesnikov S.I. Kinetic modeling of FCC process, Catalysis Today, Volume 43, Issues 3–4, 27 August 1998, Pages 315–325.

[34] Solh E., T., Jarosch, K., de Lasa, H. Catalytic Dry Reforming of Methane in a CREC Riser Simulator Kinetic Modeling and Model Discrimination. Ind. Eng. Chem. Res. 2003; 42; 2507.

[35] Teuner, St. C. Neumann, P. Von Linde, F. The Calcor Standard and Calcor Economy Processes. Oil Gas Eur. Mag. 2001; 3; 44.

[36] Youn M. H., Seo J. G., Cho K. M., Park S., Park D. R., Jung J. C. Hydrogen production by auto-thermal reforming of ethanol over nickel catalysts supported on Ce-modified mesoporous zirconia: effect of Ce/Zr molar ratio. Int J Hydrogen Energy 2008; 33:5052–9.

[37] Aceves Olivas D.Y. Baray Guerrero M.R., Escobedo Bretado M.A., Marques da Silva Paula M., Salinas Gutiérrez J., Guzmán Velderrain V., López Ortiz A. Collins-Martínez V. Enhanced ethanol steam reforming by CO_2 absorption using CaO, CaO*MgO or Na_2ZrO_3. Int J Hydrogen Energy 2014; 39:16595–16607.

[38] Solunke R. D. and Veser G. Hydrogen Production via Chemical Looping Steam Reforming in a Periodically Operated Fixed-Bed Reactor, Ind. Eng. Chem. Res. 2010, 49, 11037–11044.